論文の内容の要旨

Construction of Catalytic Reaction Nano-spaces in a Porous Molecular Crystal, Metal–Macrocycle Framework (MMF)

（多孔性分子結晶 Metal–Macrocycle Framework (MMF) のナノ空間を用いた触媒反応場の構築）

米澤　拓孝

1. Introduction

Nano-spaces around active sites of enzymes play important roles in controlling reactions (Figure 1a). Inspired by the molecular behaviors, a variety of reaction nano-spaces with catalytic active sites have been constructed in coordination cages and porous materials which provide high specificity, efficiency, and selectivity of the reactions. However, it is still challenging to design functional nano-spaces based on multi-point and site-selective interactions between substrates and inner surfaces in such a confined nano-space.

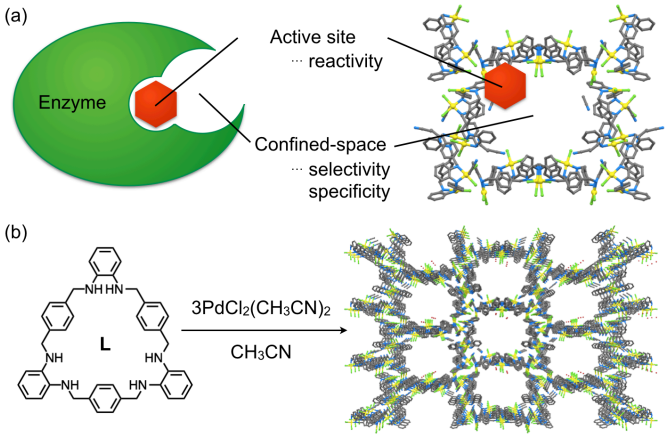

Figure 1. (a) Schematic views of active sites in a confined-space of enzyme and metal–macrocycle framework (MMF). (b) Synthesis of MMF.

A porous molecular crystal, metal–macrocycle framework (MMF), can be constructed from a macrocyclic hexaamine **L** and $PdCl_2$ (Figure 1b). MMF has one-dimensional nano-channels with a 1.4 × 1.9 nm^2 dimension, and five enantio-paired molecular binding sites are arranged on the inner surfaces. Such confined spaces with inner surfaces in MMF have high potential as catalytic reaction nano-spaces which allow highly specific, efficient, and selective reactions based on the multi-molecular adsorption with high site-selectivity.

In this study, I have constructed reaction nano-spaces with catalytic active sites in MMF for the development of space-specific reactions. Specifically, non-covalent immobilization of *p*-toluenesulfonic acid (*p*-TsOH) in MMF was conducted for a size-specific acid-catalyzed reaction. Moreover, it was found that photo-activation of the Pd centers on the surfaces of MMF channels provides an excellent platform for olefin migration reactions.

2. Non-covalent immobilization of an acid catalyst for a size-specific reaction

In my master course study, in the light of the fact that a variety of substituted benzene molecules site-selectively bind to macrocyclic cavity-derived pockets, I found that *p*-TsOH immobilized in MMF can catalyze a size-specific deprotection reaction in a preliminary experiment. Then, in my doctoral course study, I

optimized the reaction condition and quantitatively analyzed the reaction to examine the effects of the channel structure of MMF with a given dimension on the catalytic reactivity and the reusability of MMF as a heterogeneous catalyst.

The acid-catalyst, *p*-TsOH@MMF, which includes approximately 1.6 *p*-TsOH molecules per a unit-space, was prepared by soaking MMF crystals in a solution of *p*-TsOH·H_2O in acetonitrile and successive washing with dichloromethane to remove excess *p*-TsOH from the channel spaces. There was a concern that the immobilized *p*-TsOH would be dissociated from the inner surface of MMF due to the non-covalent binding. However, the catalyst was stably adsorbed to the surface during the reaction under this condition and was therefore reusable. The deprotection reactions of the trityl-protected $PhCH_2OCPh_3$ **1** and Pd-TPPCH_2OCPh_3 **2** (Pd-TPP = palladium tetraphenylporphyrinato) were compared in the presence of a catalytic amount of *p*-TsOH@MMF possessing channels with a 1.4 × 1.9 nm^2 dimension. The reaction proceeded with the smaller **1** in up to 70% yield, whereas no reactions were observed with the larger **2** even after three weeks (Figure 2). This result indicates that only the substrate incorporated in the channel can be catalyzed in a highly size-specific manner.

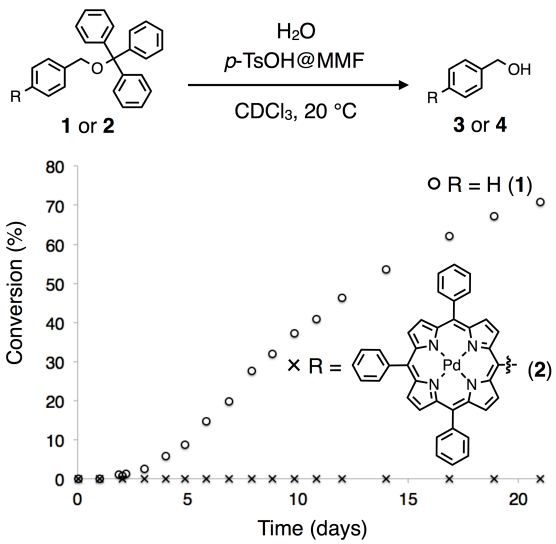

Figure 2. Time course analysis of deprotection reaction with 6 mol% of *p*-TsOH@MMF.

3. Development of photo-induced olefin migration in MMF

Stable coordination bonds often become more labile by external stimuli such as light, and generate reactive species. In this study, the Pd centers exposed to the inner space of MMF were successfully activated by light to catalyze olefin migration (Figure 3). The mechanism of this reaction was then examined both experimentally and theoretically.

The inclusion of 4-allylanisole **5** in MMF was confirmed by single-crystal X-ray diffraction and NMR measurements after soaking in a solution of **5** in acetonitrile. MMF crystals including **5** yielded an olefin-migrated product **6** quantitatively under photo-irradiation, whereas no reactions took place in the dark (Scheme 1). Moreover, even photo-irradiation around 450 nm, though more slowly, promoted the reaction. This suggests that the olefin

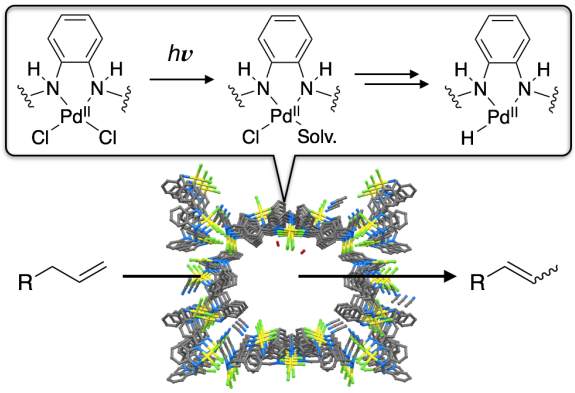

Figure 3. Schematic representation of olefin migration reaction with photo-activated Pd species.

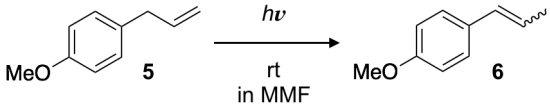

Entry	Light source (nm)	Time (h)	Yield (%)
1	280 ~ 630	2	91
2	450 ± 10	12	8
3	no irradiation	12	0

Scheme 1. Wavelength dependence of photo-induced olefin migration. The *E*/*Z* ratio was over 10.

migration be promoted by a photo-activated species generated in MMF.

Deuterated 4-allylanisole (**5**-*DD*) was used to clarify the reaction mechanism. A 1,2-D shift product **6**-*DDH* and the less deuterated product **6**-*DHH* were detected in addition to a 1,3-D shift product **6**-*DHD* (Figure 4). This result suggests that the olefin migration was catalyzed by Pd-H species *via* a well-known alkyl mechanism involving intermolecular 1,3- and 1,2-H shift mechanisms.

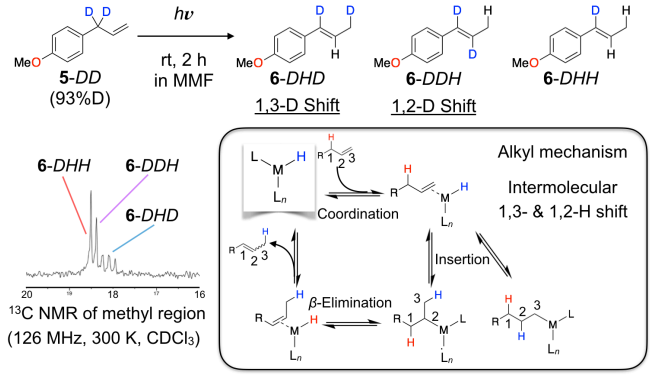

Figure 4. Deuterium labelling experiment. The inset shows a generally proposed alkyl mechanism.

Photo-activation of the Pd centers in MMF was assessed by MS-CASPT2 calculation using a model complex, a $PdCl_2$ complex of *N*,*N*′-diethyl-*o*-phenylenediamine. The vertical excitation spectrum suggests the strong absorption bands around 295 and 457 nm attributable to electron transitions toward σ^* orbital of the Pd-Cl bond. This orbital was possibly assigned to an antibonding orbital of the Pd-Cl bond, suggesting photo-cleavage by light absorption in the absorption regions. In addition, single-crystal XRD analysis before and after two-hour photo-irradiation at –180 °C was conducted for the direct observation of the Pd-Cl bond cleavage by photo-irradiation. In comparison of the electron density maps, the significant decrease in the electron density around Cl9 indicates the site-selective photo-cleavage of the Pd5-Cl9 bond (Figure 5).

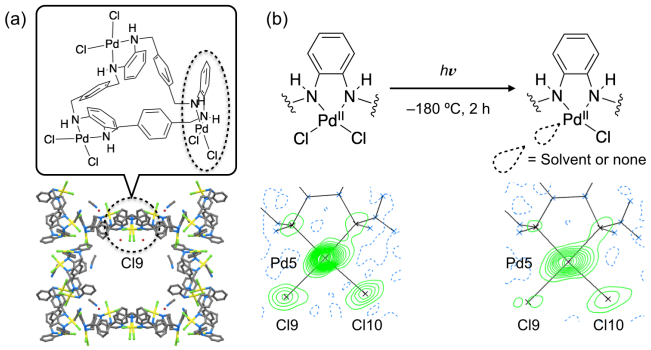

Figure 5. (a) Enlarged partial structure of MMF. (b) Direct observation of the Pd-Cl cleavage under photo-irradiation.

Taken all together, the photo-cleavage of the Pd-Cl bond of Pd centers in MMF appears to occur in a site-selective manner leading to successive formation of reactive Pd-H species, which would promote the Pd-catalyzed olefin migration *via* the alkyl mechanism.

4. A preferential photoreaction in a confined MMF nano-space

Photo-reactive substrates were expected to show a different reactivity in a confined MMF nano-space. Then, 1,6-dienes **7a** and **7b**, which normally provide an intramolecular [2+2] cycloadduct under photo-irradiation, was examined in MMF (Figure 6). 1,6-Diene **7a** in MMF was converted into an internal olefin **9a** in 20% yield under photo-irradiation, whereas **7a** in acetonitrile was converted into a [2+2]

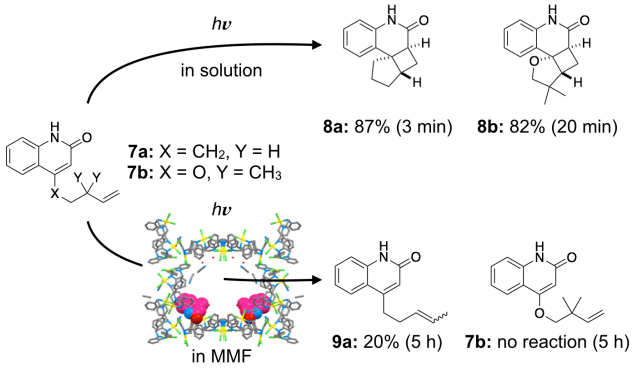

Figure 6. Comparison of the reactivity of 1,6-dienes, **7a** and **7b**, in solution and MMF.

cycloadduct **8a** in 87% yield under photo-irradiation and no olefin migration reactions took place at all. For reference, **7b** in MMF resulted in no reactions due to the presence of two methyl groups on the allylic position, whereas [2+2] cycloaddition proceeded in acetonitrile. This result indicates that the [2+2] cycloaddition of **7a** in MMF was completely inhibited and the reaction proceeded through a different pathway to form an olefin migration product.

A photo-shielding effect of MMF was then considered as a cause of inhibition. However, *cis*/*trans* photo-isomerization of azobenzene proceeded in MMF, though slowly. From a viewpoint of solvation in a confined space, a suitable conformation is required to facilitate the intramolecular [2+2] cycloaddition. As found in the model experiments, [2+2] cycloaddition was strongly suppressed in a frozen solvent (CD_3CN, –78 °C) and molecular crystals of **7a**, whereas the reaction proceeded in cooled solvents (CD_3OD and toluene-d_8, –78 °C) (Scheme 2). This result suggests that the mobility of molecules have a large effect on the [2+2] cycloaddition of **7a**. Single-crystal XRD and NMR analyses suggest that **7a** in MMF adsorbed with a high occupancy to one of the binding sites through two hydrogen bonds (Figure 7). Therefore, the inhibition of [2+2] cycloaddition can be well explained by the unfavorable binding conformation of **7a**, its restricted conformation due to the lower mobility of solvating molecules, and, though to a lesser extent, the photo-shielding effect of MMF.

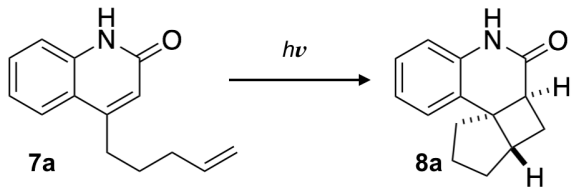

Entry	Conditions	Time (min)	Conversion (**7a**, **8a**, %)
1	in CD_3CN, rt	3	0%, 87%
2	in CD_3CN, -78 °C	120	87%, 9%
3	in molecular crystal, rt[a]	120	98%, 2%
4	in CD_3OD, -78 °C	10	0%, 91%
5	in toluene-d_8, -78 °C	10	0%, 92%

Scheme 2. [2+2] cycloaddition of **7a** in various reaction media.

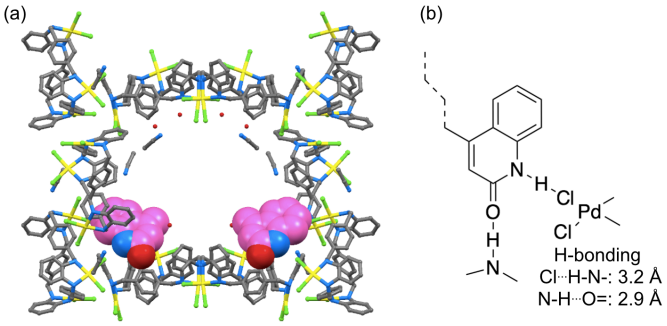

Figure 7. (a) Binding mode of **7a** to the inner surface of MMF. (b) Hydrogen-bonded interactions between **7a** and the Pd-center.

5. Conclusion

In my doctoral course study, I have established efficient ways to construct catalytic reaction nano-spaces by introducing active sites into confined MMF nano-spaces. A size-specific reaction depending on the channel dimension has been achieved by non-covalent immobilization of an acid catalyst to the inner surface of MMF. Moreover, a Pd-catalyzed olefin migration reaction was realized by the photo-activated Pd centers in MMF forming reactive Pd-H species. Here, the spatial effects of MMF nano-spaces on the chemical reactions were discussed from the viewpoints of the molecular mobility as well as the photo-shielding effect of MMF. Such nano-spaces based on the self-assembly of functional macrocycles would lead to more precisely designed catalytic reaction centers with a different chemical reactivity from those in bulk solvents.